Study and Characterization on the Nanocomposite Underfill for Flip Chip Applications

Yangyang Sun, *Student Member, IEEE*, Zhuqing Zhang, *Member, IEEE*, and C. P. Wong, *Fellow, IEEE*

***Abstract*—The nanosilica filled composite is a promising material for the no-flow underfill in flip-chip application. However, as the filler size decreases into the nano length scale, the rheological, mechanical, and thermal mechanical properties of the composite change significantly. The filler–filler and filler–polymer interactions have a profound impact on the material properties. The purpose of this paper is to achieve an in-depth understanding of the effect of the filler size and surface treatment on material properties and therefore to design a nanocomposite formulation with desirable material properties for no-flow underfill applications.**

Mono-dispersed nanosilica filler of 100 nm in size were used in this study. An epoxy/anhydride mixture was used as the base resin formulation. The nanosilica fillers were incorporated into the resin mixture to different filler loadings from 5 wt% to 40 wt% with or without silane coupling agents as the surface treatment. UV-Visible spectroscopy showed that the underfills with nano-size filler were transparent in the visible region even at high filler loading. The curing behavior and the Tg of the nanocomposite were studied using a modulated differential scanning calorimerter. It was found that the presence of the nanosilica could hinder the curing reaction, especially at the late stage of cure. The Tgs of the nanocomposites with untreated silica were found to decrease with the increasing filler loading. The measurement of the dynamic moduli from dynamic mechanical analyzer indicated that there was a secondary relaxation related to the filler–polymer interface. The coefficient of thermal expansion of the nanocomposite was measured using a thermal mechanical analyzer. The rheology of the nanocomposite was studied using a stress rheometer. It was found that the filler treatment could significantly reduce the viscosity of the nanocomposite and improve the processing capability of the underfill. Density measurements and moisture absorption experiments both indicated that the addition of nanosilica could increase the free volume of materials. The dispersion of the nanosilica in the cured composite materials was observed using scanning electron microscopy. Control samples with micron-size silica fillers were formulated and characterized for comparison.

***Index Terms*—Electronic packaging, flip chip, nanocomposite, no-flow, silica, underfill.**

I. Introduction

THE introduction of well-dispersed inorganic particles into a polymer matrix has been demonstrated to be extremely effective in improving the performance of the polymer composites. Because of the exceptionally low coefficient of thermal expansion (CTE) of silica (SiO_2), which is only 0.5 ppm/°C, the silica filled composite materials have attracted much attention to reduce the CTE of polymer composites and to improve the mechanical properties. A typical example of a silica-filled polymer composite in microelectronics applications is the underfill. Underfill is a layer of adhesive that is applied between the chip and the substrate to alleviate thermal mechanical stress on the solder joints in the flip-chip package [1]. Silica is used as the filler to reduce the CTE of underfill so as to match the CTE of the solder material to achieve high reliability [2]. In conventional underfills, the size of the silica fillers is in the micrometer range, and traditional methods such as shearing and milling can be used to achieve high filler loading level. With the fast development of the electronics industry, electronics products are becoming smaller, faster, and less expensive with more functionality and better performance. Underfill technology has evolved as well to meet the demand of decreasing feature size and increasing input/output (I/O) number in the integrated circuit (IC) chip. New technologies such as no-flow underfill and wafer level underfill have been invented to replace the conventional capillary flow underfill and to reduce the cost of the flip-chip [3]. In the no-flow underfill process, as schematically displayed in Fig. 1, the underfill material is dispensed on the substrate. Then the IC chip is placed onto the substrate, and the whole assembly is subjected to solder reflow. The underfill materials are cured during the same process. This technique simplifies the flip-chip underfill process by eliminating separate flux application and cleaning steps, avoiding time-consuming underfill capillary flow, and combining solder reflow and underfill curing into one step. Thus, the no-flow underfill process can greatly improve the production efficiency of the flip-chip assembly.

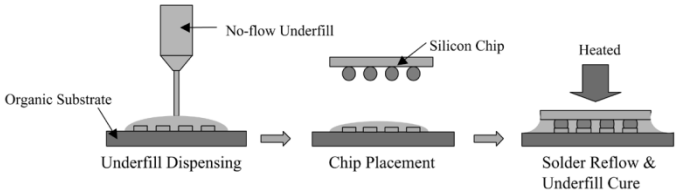

Fig. 1. No-flow underfill process.

Since the no-flow underfill is applied prior to the placement of the IC chip, conventional micron-size fillers have a great propensity of being entrapped between the solder bumps on the chip and the contact pads of the substrate [4]. The trapped fillers prevent solder wetting on contact pads and thus significantly reduce the solder joint yields. Another problem related to the underfill filled with micron-size silica is that it becomes opaque at high filler loading due to light scattering. This introduces diffi-

Manuscript received February 26, 2004; revised April 8, 2005. This work was supported in part by the National Science Foundation under Grant DMI-0 217 910, by the Packaging Research Center, Georgia Institute of Technology, and by Lindau Chemicals. This work was recommended for publication by Associate Editor R. Chanchani upon evaluation of the reviewers' comments.

Y. Sun and C. P. Wong are with the School of Materials Science and Engineering, Packaging Research Center, Georgia Institute of Technology, Atlanta, GA 30332 USA (e-mail: cp.wong@mse.gatech.edu).

Z. Zhang is with the Imaging and Printing Group, Hewlett-Packard Company, Corvallis, OR 97330 USA.

Digital Object Identifier 10.1109/TCAPT.2006.

culty in vision recognition during the chip placement since the underfill covers the bond pads on the substrate.

With the advancement in nano-science and nano-technology, the production of nanosilica through the sol gel process has been widely used in both scientific research and engineering development. Researchers [5] have found that the nanosilica in the size region of 100 to 150 nm do not tend to settle in the resin and the resulting nanocomposite material does not suffer from the filler entrapment in the flip-chip assembly. Gross *et al.* [6] demonstrated a successful flip chip assembly with no-flow underfill filled with nanosilica. The thermal cycling data showed the nanocomposite underfill had the potential to achieve a significant reliability enhancement. However, as the filler size decreases into the nano level, the rheological, mechanical, and thermal mechanical properties of the composites change significantly. Nano-size silica is known to agglomerate easily due to its high surface area and hydrophilic surface property. As such, the viscosity of the nanocomposite underfill tends to be high, which makes it impossible to achieve high filler loading with good flow ability of liquid underfill. Chemical treatment of nanoparticle surface is necessary to improve the compatibility between the nanofiller and the resin, so as to decrease the viscosity of the underfill.

In this paper, nanosilica with and without surface treatment were used as fillers in no-flow underfills. The rheological, optical, physical, thermal mechanical properties, and curing behaviors of these materials were studied in comparison to the control samples with micron-size silica filler. The objective of this study was to elucidate the filler–filler and filler–polymer interactions in the composites and to achieve an in-depth understanding of the effect of the filler size and surface chemistry on the underfill material properties.

II. Experiments

Silica nanoparticles (SiO_2, 100 nm average diameter) were commercially available and used as-received or treated with silane additives. For comparison, conventional silica with a 3-μm average diameter was also used as filler. The epoxy used was diglycidyl ether of Bisphenol-A type (EPON828, from Shell Chemicals with an average molecular weight of 377). The hardener was hexahydro-4-methylphthalic anhydride (HMPA, from Lindau Chemicals). A polymer-encapsulated imidazole derivative from Shikoku Chemicals was used as a latent catalyst. γ-glycidoxypropyl-trimethoxysilane (GPTMS) and surface-active additive tetra-n-butyl titanate (TnBT) were used as the silica modification compounds into the underfills. All of these chemicals were used as received.

The base polymer formulation was prepared by mixing EPON828 and HMPA with a weight ratio of 1:0.75. After stirring the polymer mixture for 10 min, the catalyst, with 1 wt% based on the polymer mixture, was added into polymer liquid and stirred for another 30 min until a homogenous polymer solution was achieved. A specified quantity of filler was added into the base polymer and the mixture was sonicated for 30 minu using a Sonicator (Misonix 3000) at a power of 450 W. To treat the nanosilica surface, 3 wt% silane GPTMS and 1 wt% TnBT based on silica filler were added and the mixture was sonicated for another 5 min. All the samples were named according to their filler nature and loading. For example, "treated-30" means an underfill sample with 30 wt% surface-treated nanosilica, and "3 μm-30" means that with 30 wt% micron silica. The filler loading of the composite was 5%, 10%, 20%, 30%, and 40% in weight percent.

The viscosity of the underfills at room temperature was studied using a stress rheometer (TA Instruments, AR1000N) in a steady flow mode. A cone-and-plate geometry was used. A liquid underfill sample was dispensed on the plate before the run and the experiments were conducted with a stepped shear rate from 0.01 to 100 s^{-1}.

Light absorption measurements of underfills were made on a UV-Visible spectrophotometer (Beckman Du520). To prepare the sample, the liquid composite underfill was coated on the quartz glass slide with a thickness of 25 μm. Then the specimen was put into the chamber of the UV–Vis spectrophotometer and scanned from 350 nm to 750 nm which included the visible region.

The curing behavior and glass transition temperature of the epoxy composites were characterized by a modulated differential scanning calorimeter (DSC, TA Instruments, Model 2920). A sample of approximately 10 mg was sealed in a hermetic aluminum pan. A dynamic scanning experiment was conducted with a ramp rate of 5 °C/min, from ambient temperature to 300 °C, to obtain the curing heat flow diagram of the composite. The cured sample was left in the DSC cell and cooled to room temperature. Then the sample was reheated to 200 °C at 5 °C/min to obtain another heat flow diagram. The initial temperature of the heat flow step of the second diagram is defined as the DSC glass transition temperature (DSC Tg).

In order to evaluate bulk properties of the composite samples after curing, the liquid filler-polymer mixture was poured into an aluminum dish and cured in the convection oven at 150 °C for 1 h and 180 °C for another 2 h.

A dynamic mechanical analyzer (DMA, TA Instruments, Model 2980) was used to measure the dynamic moduli and glass transition temperature of the composites. The cured sample was cut into a strip with dimensions of about $18 \times 6 \times 2$ mm. The test was performed in a single cantilever mode. The temperature was increased from room temperature to 250 °C at a heating rate of 3 °C/min, while the storage modulus (E'), loss modulus (E") and $\tan\delta$ were calculated by the pre-installed software. The DMA Tg was determined by the corresponding peak of the loss modulus (E") curve.

The coefficient of thermal expansion (CTE) of the cured sample was measured on a Thermomechanical analyzer (TMA, TA Instruments, Model 2940). The dimensions of the sample were about $5 \times 5 \times 2$ mm. The sample was heated in the TMA furnace at 5 °C/min from room temperature to 200 °C. The CTE before the Tg is defined as α_1 and after the Tg as α_2.

The density was measured by using the Archimedes approach [7], [8], where the cured sample was weighed in air and then in water using a balance with a reproducibility of better than 0.5 mg. The average of measurements of at least three specimens was reported for each sample.

The cured underfill was subjected to temperature/humidity aging at 85 °C and 85% RH. The sample was taken out of the aging chamber and the increased weight due to moisture uptake was recorded daily.

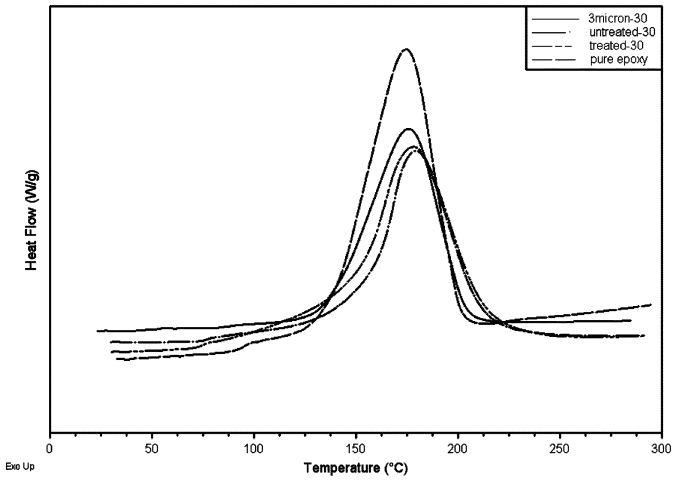

Fig. 2. Curing behaviors of base underfills and composite by DSC.

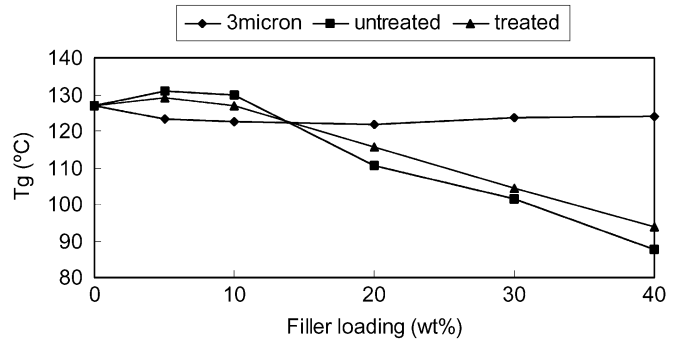

Fig. 3. Glass transition temperatures of composite underfills by DSC.

The dispersion of the nanosilica in the cured composite materials was observed using a scanning electron microscope (SEM Hitachi S800). A preliminary wetting test was performed using a eutectic SnPb solder bumped quartz chip and a Cu substrate. The bumps were area-array distributed; the diameter of the bumps was 75 μm. The no-flow underfill was first dispensed on the Cu board, followed by the placement of the quartz chips on the underfill. Then the assembly was subjected to the standard eutectic SnPb solder reflow process. The wetting of the solder on the copper board was observed using an optical microscope.

III. Results and Discussions

A. Curing Behaviors and Tg of Composite Underfills

The curing behaviors of composite underfills were characterized by DSC dynamic heating experiments. The curing profiles of a underfill with 30 wt% silica, including micron silica, untreated nanosilica and treated nanosilica, are shown in Fig. 2. For comparison, the underfill without silica is also included in the figure. As can be seen from Fig. 2, the micron size fillers did not affect the curing process of the epoxy resin. However, the presence of the nanosilica could inhibit the curing reaction, especially at the late stage of cure. Both treated-30 and untreated-30 samples had a delayed "tail" in the curing curves. For the development of nanocomposite underfills, the cure inhibition effect caused by nanosilica could bring a negative effect to the underfill process since it needs longer post-cure time.

Fig. 3 shows the DSC Tg of silica composite underfills. It can be observed from the graph that the addition of nanosilica can decrease the Tg of the composite appreciably while the micron-size fillers does not have a significant effect on the Tg of the composites. The Tg of untreated-40 sample was almost 40 °C lower than that of the pure epoxy. On the other hand, silane treatment on the fillers could increase the Tg of the nanocomposites by several degrees at high loading levels. The Tg depression in nanocomposites might be due to two reasons. First, nano-size filler can inhibit the curing reaction as mentioned before, resulting in a lower crosslinking density in the epoxy matrix and therefore has a lower Tg. Second, nanosilica has a much larger surface area and interfacial interaction with epoxy matrix than the micron silica. The large filler-resin interface creates extra free volume leading to a lower Tg. The silane treatment on the silica surface improves the compatibility between the fillers and the resin, which decreases the free volume at the interface and therefore slightly increases Tg.

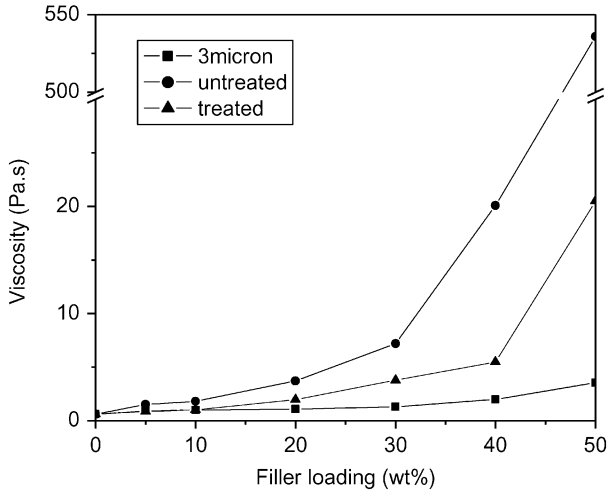

Fig. 4. Viscosity of silica filled composite underfills.

B. Rheological and Optical Behavior of Composite Underfills

Fig. 4 shows the viscosity of the composite underfills at room temperature as a function of filler loading with 3-μm, nano-treated and nano-untreated silica fillers. As can be seen from the figure, the addition of nanosilica filler can significantly increase the underfill viscosity, especially at high filler loading. The viscosity of the underfill with 50 wt% nano-size filler exceeded 500 Pa$\cdot$s, more than 100 times higher than the one with 50 wt% micron-size filler. This brings a great challenge to process and apply the nanosilica filled composite underfills in no-flow underfill assembly. Results also showed that the surface treatment on the nanosilica surface would enhance the compatibility between the filler and the epoxy matrix and lower the viscosity of the composite material. The underfill with surface treated nanosilica had a significantly lower viscosity at high filler loading than the one without surface treatment. The silica surface modification is an effective way to reduce the viscosity of the nanosilica composite underfill and to improve their processing compatibility.

The light absorption property of composite underfills with different filler size is shown in Fig. 5. The transmittance of light in the visible region decreased greatly with the 3-μm silica fillers while composite underfills with nano-size silica

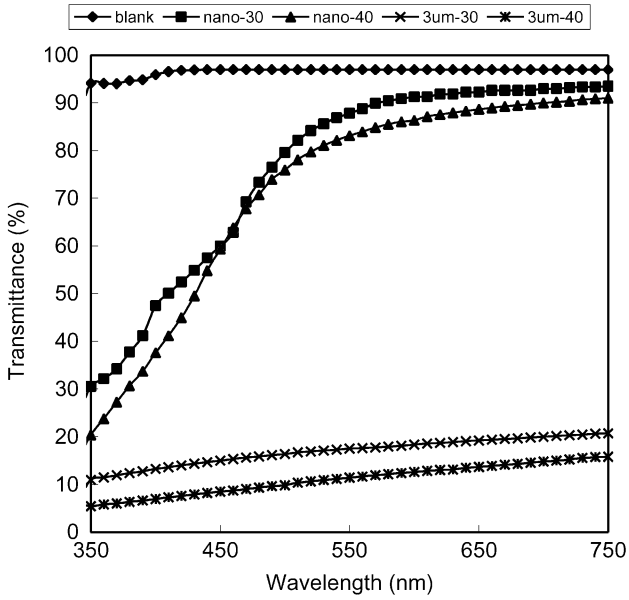

Fig. 5. Effect of filler size on the UV-Vis spectra of the composite underfills.

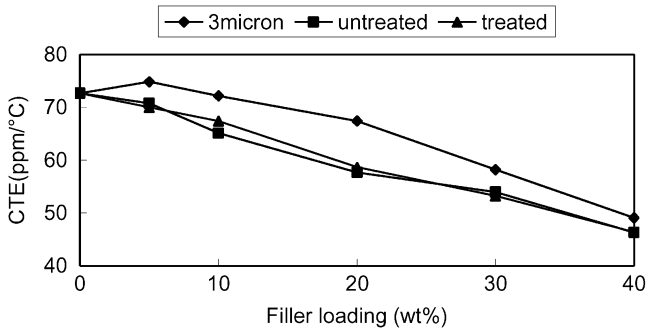

Fig. 6. CTE of silica filled composite underfills.

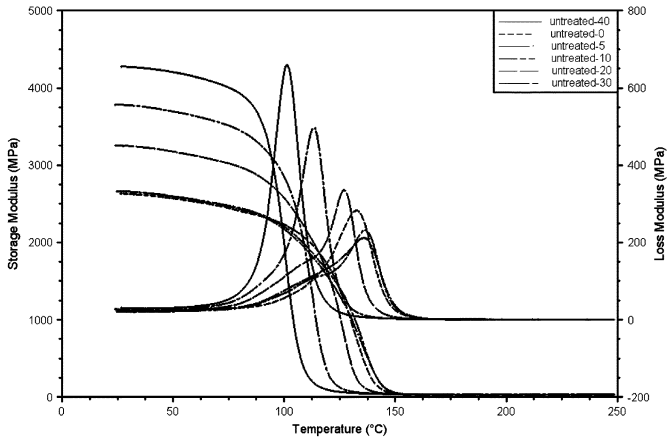

Fig. 7. Dynamic moduli of composite underfills with untreated nanosilica.

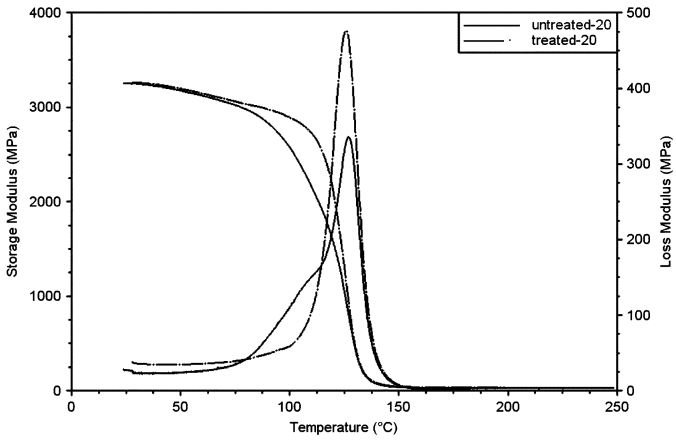

Fig. 8. Comparison of dynamic moduli of composite underfills with different nanosilica.

were almost as transparent as pure epoxy in visible region (400–700 nm). Since no-flow underfill is pre-applied on the substrate before chip placement, an optically transparent liquid is desired for vision recognition during the chip placement process. The underfill filled with micron-size silica becomes opaque at high filler loading due to light scattering. This introduces difficulty in the chip placement since the underfill covers the bonding pads on the substrate. Nanosilica filled underfill, on the other hand, is transparent to visible light because the filler has a particle size smaller than the wavelength of the visible light. The nanosilica composite underfills provide unique optical properties for chip assembly application.

C. Thermal Mechanical Properties

The primary purposes of loading silica filler into no-flow underfill are to reduce the coefficient of thermal expansion (CTE) and to increase the elastic modulus. These two thermal mechanical properties are critical parameters to the thermomechanical reliability of a flip-chip package [9]. Fig. 6 shows the CTE value of composite underfills as a function of filler loading. For all three kinds of filler, the CTE decreased almost linearly as the filler loading increased. There was no obvious difference in CTE value for underfill with untreated and silane treated nanosilica. It was found that the CTE of the composite not only depended in the silica loading, but also the silica size [10]. Some literature showed that the CTE of composite underfills could reduce from 40 ppm/°C to 26 ppm/°C as the filler size decreased from 30 μm to 7 μm at 70 wt% filler loading. This experiment also indicated that the CTE of underfill with nanosilica is smaller than that with 3 μm filler at the same loading level. This is because the interface of the filler particles and the resin matrix constricts the expansion of the epoxy matrix. Therefore, an increase in the constriction of the matrix due to increased surface area of the nanosilica allows a decrease in the expansion of the matrix.

Fig. 7 shows the dynamic moduli of underfill with untreated nanosilica measured by DMA. The Tg of the underfill measured by peak temperature of loss modulus showed the same trend as observed in the DSC experiment; it decreased as filler loading increased. However, at low filler loading (5, 10, and 20 wt%), the loss modulus showed a secondary relaxation process below the glass transition, possibly related to the surface relaxation at the resin-filler interface. As the filler loading increased, this secondary relaxation overlapped with the glass transition. In other words, with the increase of the interface between the filler and the resin, the surface relaxation became dominant and reduced the Tg of the composite. Fig. 8 shows the comparison of dynamic moduli for underfills with the treated and untreated

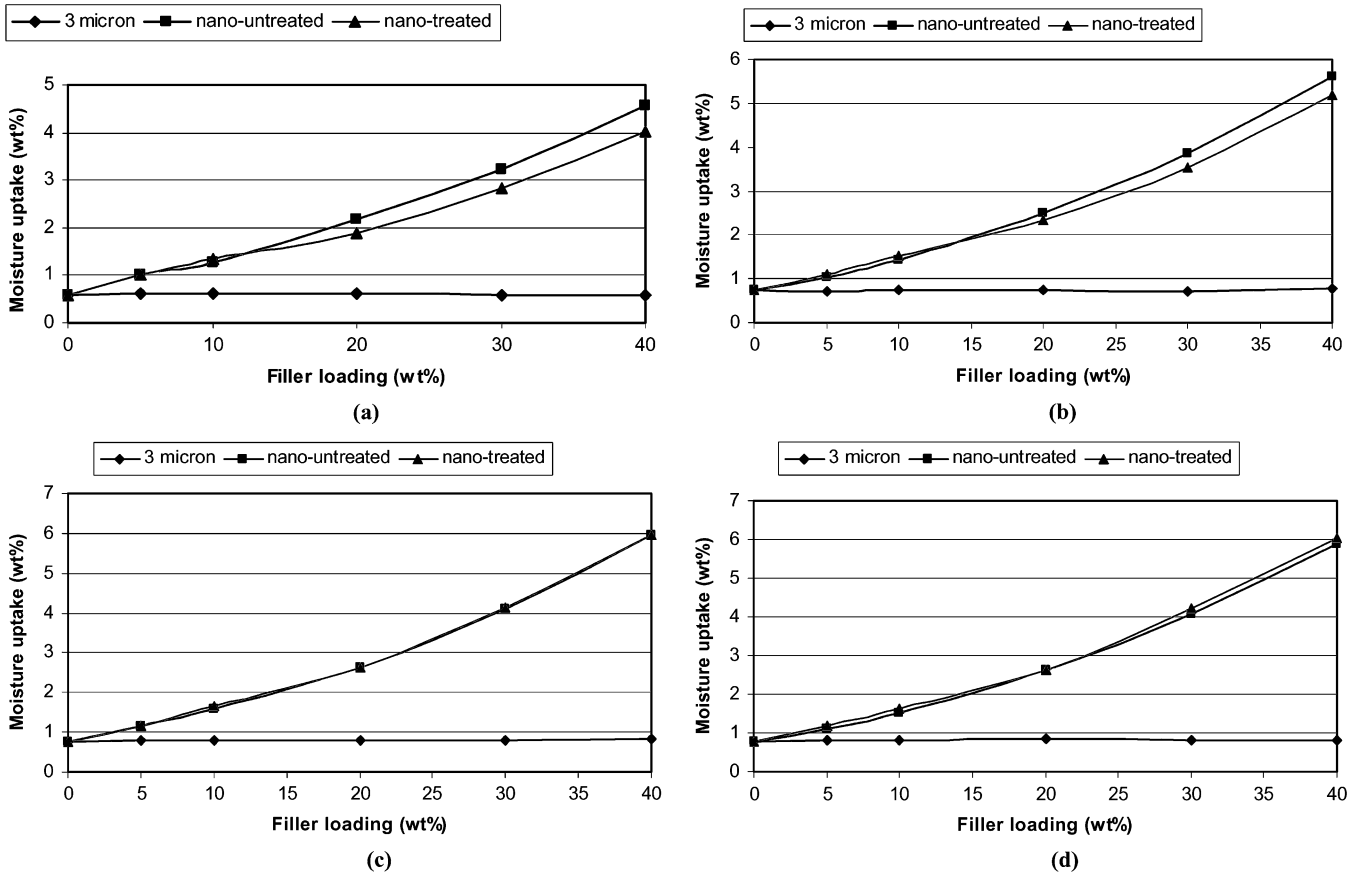

Fig. 9. Moisture uptake evaluations for underfill with different silica: (a) one day, (b) two days, (c) three days, and (d) four days.

20 wt% nanosilica. Unlike the untreated-20 nanosilica composite, the secondary relaxation below the glass transition was not observed in the loss modulus of the treated-20. It is possible that the silane treatment alters the interfacial properties and improves the compatibility of the resin-filler interface.

D. Moisture Absorption and Density Measurement

Silica composite underfills were also characterized in term of moisture absorption. The cured underfills were subjected to temperature/humidity aging at 85 °C and 85% RH. With the assumption that all the weight increasing during the 85 °C/85% RH aging was due to the water absorption in the polymer, the moisture uptake was normalized to polymer weight percentage. Fig. 9 shows the evaluation of moisture uptake in underfills with aging time. As can be seen from Fig. 9, micron-size filler did not alter the moisture absorption behavior of the polymer matrix. However, the nano-size filler increased the moisture absorption due to the additional free volume at the interface. As filler loading increased, the effect became more prominent.

Generally, moisture absorption processes in polymer composites can be described by Fick's second law of diffusion, which can be expressed as [11]

$$\frac{M_t}{M_\infty} = 1 - \frac{8}{\pi^2} \sum_{n=0}^{\infty} \frac{1}{(2n+1)^2} \exp\left\{ \frac{-D(2n+1)^2 \pi^2 t}{h^2} \right\} \quad (1)$$

where M_t and M_∞ are the moisture content at time t and the equilibrium or maximum moisture content, respectively. D is the diffusion coefficient and h is the sample thickness.

At short times (i.e., the initial absorption), (1) can be reduced to

$$\frac{M_t}{M_\infty} = 4 \left(\frac{Dt}{\pi h^2} \right)^{0.5} \quad (2)$$

which can be rewritten as

$$M_t = k t^{0.5} \quad (3)$$

where k is a rate constant relating to the diffusion coefficient.

To elucidate this phenomenon clearly, the moisture absorption of underfills with 30 wt% filler as a function of time before moisture saturation is shown in Fig. 10. The moisture absorption kinetics was also calculated according to the (3). It can be seen that surface treatment of nanosilica slowed the rate of moisture uptake in the composites. The samples with both treated and untreated nanosilica had much higher moisture uptake and faster absorption rate than the pure polymer and micron-sized composite. The parameters for (3) were listed in Table I for four samples, which also indicated the different

The experiments on moisture absorption showed that the incorporation of nano-size filler into the polymer matrix could change the free volume of polymer. In order to verify the difference of free volume at glassy state, a density measurement was

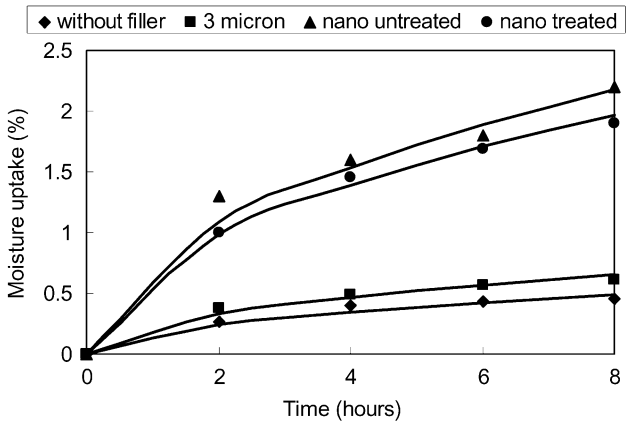

Fig. 10. Kinetics of moisture uptake for the samples.

TABLE I
MOISTURE ABSORPTION KINETICS PARAMETER

Materials	*without filler*	*micron filler*	*untreated nanosilica*	*treated nanosilica*
k (rate constant)	0.1727	0.2319	0.7694	0.6963

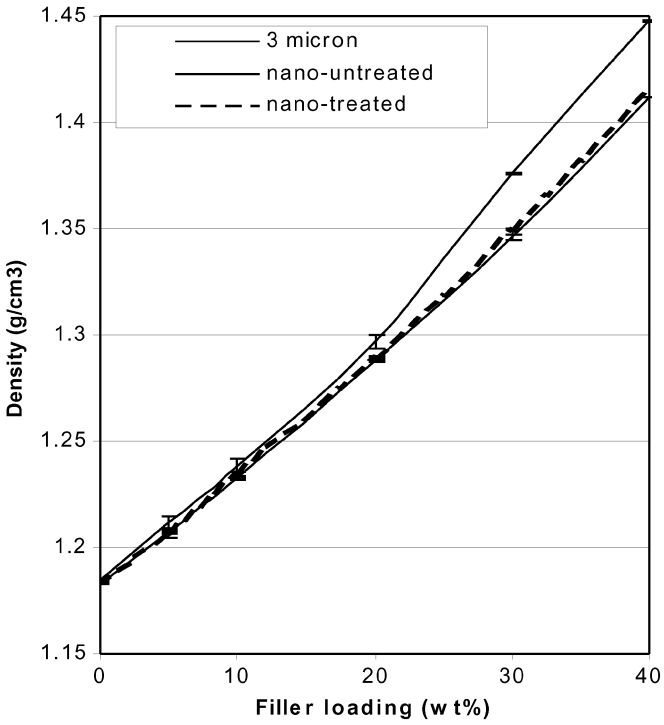

Fig. 11. Density measurement for silica filled composite underfills.

conducted for composite underfills. The influence of the silica content and size on the density of the composite underfills is shown in Fig. 11. It can be seen that the density of the composites with 3-μm silica was higher than that with nanosilica. This difference was much more evident at the high filler loading. These results are consistent with the moisture absorption and glass transition temperature experiments, i.e., the nano-size silica can change the free volume of polymer in composites,

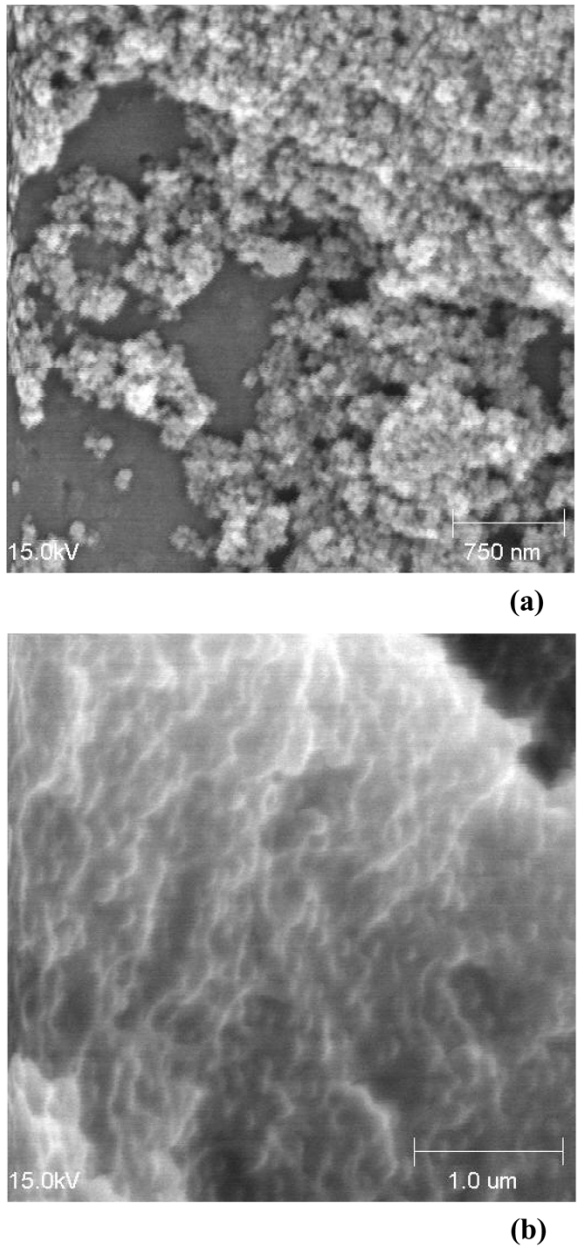

Fig. 12. SEM photographs of nanosilica composite materials: (a) untreated-30 and (b) treated-30.

so the nanocomposites show a lower density, higher moisture absorption and lower Tg than micron-size filled composites. The density of the nano-treated sample was slightly higher than that of the nano-untreated. This means that silane modification to nanosilica can improve the compatibility of the silica and polymer phases and thus result in a more "compact" composite structure and less free volume in the polymer.

E. Morphology

To investigate the dispersion of nanosilica in the epoxy matrix, the cured composite materials were polished carefully to get a very reflective surface. The thin sections of polished surface were cut and mounted on an aluminum stub using a conductive tape and were sputter-coated with gold before the cross-section examination. Fig. 12 shows the SEM photographs of cured

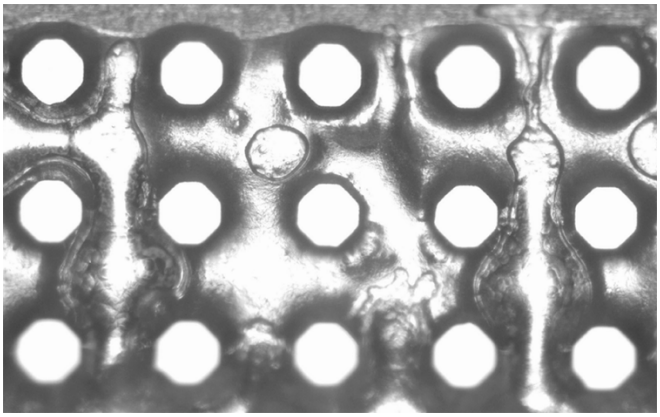

Fig. 13. Wetting picture of quartz chip with treated-30 underfill.

underfill with 30 wt% treated and untreated nanosilica, respectively. The nanosilica without silane treatment formed large agglomerations and obviously phase separated from the polymer matrix, as shown in Fig. 12(a), while after silane treatment, the nanosilica kept even mono-dispersion in the polymer matrix without large aggregation, as shown in Fig. 12(b). This serves as direct evidence that the silane treatment can change the silica surface properties and improve the compatibility between silica and epoxy, so nano-treated samples have tighter integration of the inorganic-organic phase and less interfacial interaction between nanosilica and epoxy than nano-untreated ones. The disadvantages with small size and large surface area of nanosilica, which greatly influence the composite material properties, can be overcome by silane treatment of the nanosilica surface, as indicated by previous experimental results.

F. Wetting Test

A preliminary wetting test was carried out with 30 wt% treated nanosilica underfill using quartz chips and clean laminated FR-4 board. A fluxing agent was added to the underfill to eliminate the surface oxide on the solder. Fig. 13 shows the top view of the test coupon. The solder balls on the quartz chip wet well on the copper board below with the fluxing of the underfill. The incorporation of treated nano-size silica did not hinder the formation of the solder joint between the quartz chip and the copper board. This indicates that surface modified nanosilica composite can be used as no-flow underfill.

IV. Conclusion

Nanosilica composite underfills were prepared and characterized for their curing behaviors and physical, optical, rheological and thermal mechanical properties. Compared with micron-size silica, nanosilica would not interfere with the solder joint formation in the no-flow process, and it was transparent to visible light, which can benefit the flip chip assembly. Additionally, the CTE of nanosilica filled underfill was lower than that filled with micron silica at same loading level. However, nano-size filler also had some negative effects on the underfill materials due to large surface areas and interfacial interactions, including reducing the composite Tg, inhibiting the epoxy curing, extremely high viscosity at high loading level, high moisture absorption, and low density.

However, the results also showed that the compatibility between nanosilica and the epoxy matrix was greatly enhanced by silane modification of the nanosilica surface. Therefore, drawbacks caused by the incompatible interface between nanosilica and the epoxy matrix can be overcome.

References

[1] C. P. Wong, S. Luo, and Z. Zhang, "Flip the chip," *Science*, vol. 290, pp. 2269–2279, 2000.

[2] S. G. Konsowski and A. R. Helland, *Electronics Packaging of High Speed Circuitry*. New York: McGraw-Hill, 1997, ch. 3.

[3] C. P. Wong and S. H. Shi, "No-flow underfill of epoxy resin, anhydride, fluxing agent and surfactant," U.S. Patent 6 180 696, Jan. 30, 2001.

[4] S. H. Shi and C. P. Wong, "Recent advances in the development of no-flow underfill encapsulants—A practical approach toward the actual manufacturing application," *IEEE Trans. Electron. Packag. Manufact.*, vol. 22, no. 4, pp. 331–339, Oct. 1999.

[5] K. Gross, S. Hackett, D. Larkey, W. Schultz, and W. Thompson, "New materials for high performance no-flow underfill," in *Proc. Int. Symp. Microelectron.*, Denver, CO, Sep. 2002, pp. 234–238.

[6] K. Gross, S. Hackett, W. Schultz, and W. Thompson, "Nanocomposite underfills for flip-chip applications," in *Proc. 53th Electron. Comp. Technol. Conf. (ECTC'03)*, New Orleans, LA, May 2003, pp. 951–956.

[7] *Standard Test Methods for Density and Specific Gravity (Relative Density) of Plastics by Displacement*, Std. D792-91, 2000.

[8] M. Celina, K. T. Gillen, J. Wise, and R. L. Clough, "Anomalous aging phenomena in a crosslinked polyolefin cable insulation," *Rad. Phys. Chem.*, vol. 48, no. 5, pp. 613–626, 1996.

[9] *Microelectronics Packaging Handbook*, Chapman&Hall, New York, NY, 1997. Tummala, R., *et al.*.

[10] J. Qu and C. P. Wong, "Effective elastic modulus of underfill material for flip-chip applications," *IEEE Trans. Comp. Packag. Technol.*, vol. 25, no. 1, pp. 53–55, Mar. 2002.

[11] J. Wan, Y. L. Wang, G. X. Cheng, and K. Y. Han, "Three-dimensionally braided carbon fiber-epoxy composites, a new type of materials for osteosynthesis devices," *J. Appl. Polym. Sci.*, vol. 85, pp. 1021–1039, 2002.

Yangyang Sun (S'01) received the B.S. and M.S. degrees from Shanghai Jiao Tong University, Shanghai, China, in 1998 and 2001 respectively, and is currently pursuing the Ph.D. degree at the Georgia Institute of Technology, Atlanta.

Her research focuses on the application of nanocomposite materials in electronics packaging.

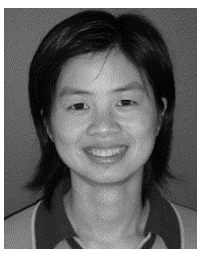

Zhuqing Zhang (M'04) received the B.S. degree from Fudan University, Shanghai, China, in 1997 and the M.S. and Ph.D. degrees from the School of Materials Science and Engineering, Georgia Institute of Technology, Atlanta, in 2001 and 2003, respectively.

She is currently an Electrical/Hardware Engineer with the Imaging and Printing Group, Hewlett-Packard Company, Corvallis, OR.

Dr. Zhang received the Georgia Tech Sigma Xi Outstanding M.S. Thesis Award in 2002, the Sigma Xi Best Ph.D. Thesis in 2004, and the 10th Annual Motorola-IEEE/CPMT Society Graduate Student Fellowship for Research in Electronic Packaging in 2002.

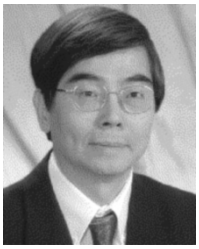

C. P. Wong (SM'87–F'92) received the B.S. degree in chemistry from Purdue University, West Lafayette, IN, and the Ph.D. degree in organic/inorganic chemistry from Pennsylvania State University, University Park.

He is a Regents' Professor and the Charles Smithgall Institute Endowed Chair at the School of Materials Science and Engineering, Georgia Institute of Technology, Atlanta. After his doctoral study, he was awarded a two-year postdoctoral fellowship with Nobel Laureate Professor Henry Taube at Stanford University, Stanford, CA. He joined AT&T Bell Laboratories in 1977 and became a Senior Sember of the Technical Staff in 1982, a Distinguished Member of the Technical Staff in 1987, and was elected an AT&T Bell Lab Fellow in 1992. Since 1996, he has been a Professor at the School of Materials Science and Engineering, Georgia Institute of Technology. He was named a Regents' Professor in July 2000, elected the Class of 1935 Distinguished Professor in 2004 for his outstanding and substained contributions in research, teaching and services, and named holder of the Georgia Tech Institute Endowed Chair in 2005. He holds over 50 U.S. patents, numerous international patents, and has published over 500 technical papers. His research interests are in the fields of polymeric materials, materials reaction mechanism, IC encapsulation, in particular, hermetic equivalent plastic packaging, electronic manufacturing packaging processes, interfacial adhesions, and nano functional material syntheses and characterizations. He is one of the pioneers who demonstrated the use of organic polymers as device encapsulant to achieve reliability without hermeticity in plastic IC packaging, elucidated the fundamental conductivity fatigue of conductive adhesives for lead-free interconnects, syntheses, and characterizations of nano lead-free alloys, developed the first no flow underfill for low cost flip-chip, ultra high k capacitor composites and novel lotus effect coating materials.

Dr. Wong received the AT&T Bell Labs Fellow Award in 1992, the IEEE CPMT Society Outstanding and Best Paper Awards in 1990, 1991, 1994, 1996, 1998, and 2002, the IEEE CPMT Society Outstanding Sustained Technical Contributions Award in 1995, the Georgia Tech Sigma Xi Faculty Best Research Paper Award in 1999, the Best M.S., Ph.D., and undergraduate Theses Award in 2002 and 2004, respectively, the University Press (London) Award of Excellence, the IEEE Third Millennium Medal in 2000, the IEEE EAB Education Award in 2001, the IEEE CPMT Society Exceptional Technical Contributions Award in 2002, elected as holder of the Charles Smithgall Institute Endowed Chair at Georgia Tech in 2005, and the IEEE CPMT Field Award in 2006. He is a Fellow of AIC and AT&T Bell Labs and a member of the National Academy of Engineering. He was the Technical Vice President (1990 and 1991) and the President of the IEEE CPMT Society (1992 and 1993).